British Journal of Applied Science & Technology
4(30): 4263-4279, 2014

SCIENCEDOMAIN *international*
www.sciencedomain.org

Influence of $NiCl_2/CdCl_2$ as Mixed Filler on Structural, Thermal and Electrical Properties of PVA/PVP Blend

I. S. Elashmawi[1,2*], E. M. Abdelrazek[3] and A. Y. Yassin[3]

[1]Department of Spectroscopy, Physics Division, National Research Center, Giza, Egypt.
[2]Department of Physics, Faculty of Science, Al-Ula, Taibah University, Saudi Arabia.
[3]Department of Physics, Faculty of Science, Mansoura University, 35516, Mansoura, Egypt.

Authors' contributions

This work was carried out in collaboration between all authors. Author ISE designed the study, performed the statistical analysis, wrote the protocol, and wrote the first draft of the manuscript and managed literature searches. Authors ISE, EMA and AYY managed the analyses of the study and literature searches. All authors read and approved the final manuscript.

Original Research Article

Received 26th June 2014
Accepted 25th July 2014
Published 19th August 2014

ABSTRACT

The present work is focusing on characterizing the films of poly (vinyl alcohol) (PVA) and poly (vinyl pyrrolidone) (PVP) with various mass fractions of $NiCl_2/CdCl_2$ by different techniques. XRD scans revealed the semicrystalline nature of the prepared films and demonstrated that complexation between the blend and the filler took place in the amorphous region. FT-IR and UV-visible studies confirmed these results. UV-visible analysis also revealed that the optical energy gap was affected by adding the mixed filler, indicating that there are charge transfers complexes arose in the polymer blend matrices. DSC revealed single T_g which indicates miscibility of the prepared films. The electrical conductivity was enhanced from 2.16×10^{-8} S/cm of pure blend to 1.1×10^{-4} S/cm for the blend filled with 20 wt % of the mixed filler so, From these data the prepared films can be used for rechargeable batteries.

Keywords: Polymer blends; miscibility; DSC; XRD; DC conductivity.

**Corresponding author: E-mail: islam_shukri2000@yahoo.com;*

1. INTRODUCTION

Materials with improved characteristics are produced by blending two or more polymers in order to combine their properties for certain purposes which cannot be achieved by one of them alone. Interest in studying polymer blends has considerably increased due to their industrial applications. The concept of physically blending of two polymers, in general has been adopted as a strategy for suppressing the crystallinity and enhancing the conductivity. The conventional methods for producing polymer blends are: melt blending, co-precipitation and solvent casting [1].

In order to investigate the miscibility and phase behaviour of polymers, differential scanning calorimetry (DSC) has been frequently used to determine the glass transition temperature (T_g) [2]. A miscible polymer blend would exhibit a single transition between T_g of the two components.

PVA is a semicrystalline, synthetic water-soluble polymer and has very important applications due to the role of hydroxyl groups and hydrogen bonds [3]. These hydrogen bonds assist in the formation of polymer blends. Because of its mechanical properties and both ionic and electrical conduction, it has some technological advantages in electrochemical devices, fuel cells, etc.

PVP deserve a special attention among the conjugated polymers; because of its good environmental stability, easy processability and moderate electrical conductivity. It has a broad wide range of applications such as electrochemical devices (batteries, displays) [4].

PVA/PVP blend is a potential material having a good charge storage capacity and dopant-dependent electrical properties. Their interactions have been described in many papers because of the interesting properties of the resulting blend, which combine the features of both polymers [5,6]. The use of modifiers can change the properties of PVA/PVP blend in many aspects. However, it is necessary to keep in mind the original idea of application and according to that choose the appropriate filler.

Recently, our research group focused on synthesizing polymer blend with high conductivities at room temperature to be used it in batteries such as rechargeable lithium batteries [7] and nickel/cadmium batteries as in this work.

The main goal of the present study is to prepare new composite films based on PVA/PVP blend doped with of different concentrations of equal mass fractions of $NiCl_2$ and $CdCl_2$ using casting techniques. A systematic investigation of structural, optical, morphological, thermal and electrical properties of these system are discussed by different tools and techniques.

2. EXPERIMENTALS

2.1 Materials and Samples Preparation

PVA was obtained from E-Merck (Germany) of molecular weight M_w = 14,000 and PVP from SISCO Research Laboratory Ltd. (Mumbai, India) of M_w = 40,000. Equal amount of PVA and PVP (5 gm from each polymer) by weight percent was added to double distilled water with stirring the solution at 328 K to complete dissociation. Nickel chloride ($NiCl_2$) and cadmium chloride ($CdCl_2$) were used as mixed filler. Required quantities of the two fillers (equal weight

of each other) were also dissolved in distilled water and added to the polymeric solution drop by drop. This solution was kept in oven until a suitable viscous solution is formed.

To prepare the polymeric films filled with mass fractions 0.5, 2.5, 5, 10 and 20 wt % of the mixed filler, the viscous solution was poured onto cleaned glass Petri dishes and kept in a vacuum oven at 338 K for 4 days to ensure removal of the solvent traces. After drying, the prepared films were peeled from Petri dishes and kept in vacuum desiccators until using them. Thicknesses of the obtained films were in the range of 60-120 μm and were measured by a digital micrometer (Mitutoyo no. 293-521-30, Japan).

2.2 Measurements

X-ray diffraction scans were obtained using DIANO Corporation with Cu Kα radiation (λ = 1.540 Å, the tube operated at 30 kV, Bragg's angle (2θ) in the range of 4-60º). FT-IR absorption spectra were carried out using the single beam Fourier transform infrared spectrometer (FT-IR-430, JASCO, Japan). FT-IR spectra of the samples were obtained in the spectral range of 4000-400 cm^{-1}. UV-visible absorption spectra were measured in the wavelength region of 200-600 nm using spectrophotometer (V-570 UV-VIS-NIR, JASCO, Japan). Morphology of the films was characterized by scanning electron microscope using (JEOL 5300, Tokyo, Japan), operating at 30 kV accelerating voltage. Surfaces of the samples were coated with a thin layer of gold (3.5 nm) by the vacuum evaporation technique to minimize sample charging effects due to the electron beam. The differential scanning calorimetry of the prepared films was carried out using Shimadzu DSC-50 from ambient temperature to 500ºC with a heating rate of 10ºC/min under argon atmosphere. DC electrical conductivity was measured using an insulation tester (Level type T M14) of accuracy ±0.2%.

3. RESULTS AND DISCUSSION

3.1 X-ray Diffraction Analysis

X-ray diffraction analysis has yielded much valuable information on the configuration of macromolecules, structure, orientation and size-ordered regions in the material [8]. Fig. (1) shows the X-ray diffraction spectra of pure PVA/PVP (50/50) blend and the blend filled with different concentrations of $NiCl_2$/$CdCl_2$.

From this figure, it is observed that the polymer blend exhibited a semicrystalline structure of the blend with two peaks at 2θ≈ 11.84º (assigned to PVP) and 19.68º. The main broad peak was observed at 2θ≈ 19.68º, which known as the amorphous hump, is originated from (101) plane of crystalline PVA [9]. This broad band stemmed from reflection of the amorphous region of the blended PVA/PVP.

The decrease in relative intensity with increase in broadness of the apparent peak at 19.68º of the filled samples has been observed when compared with pure polymer blend. This can be interpreted in terms of the Hodge et al. [10] criterion, which has established a correlation between intensity of the peak and the degree of crystallinity. Thus, the increase in broadness of this peak reveals increase in the amorphous regions in the samples. It is clear that, there are no new peaks appeared after adding fillers in the prepared samples spectra. This indicates the complete dissolution of the mixed filler in amorphous regions of the polymers.

From all previously results, the interaction between the filler and polymer blend results in decreasing crystallinity with rich amorphous phase. This amorphous nature is responsible for higher conductivity and confirms the complexation between the mixed filler and the polymer blend.

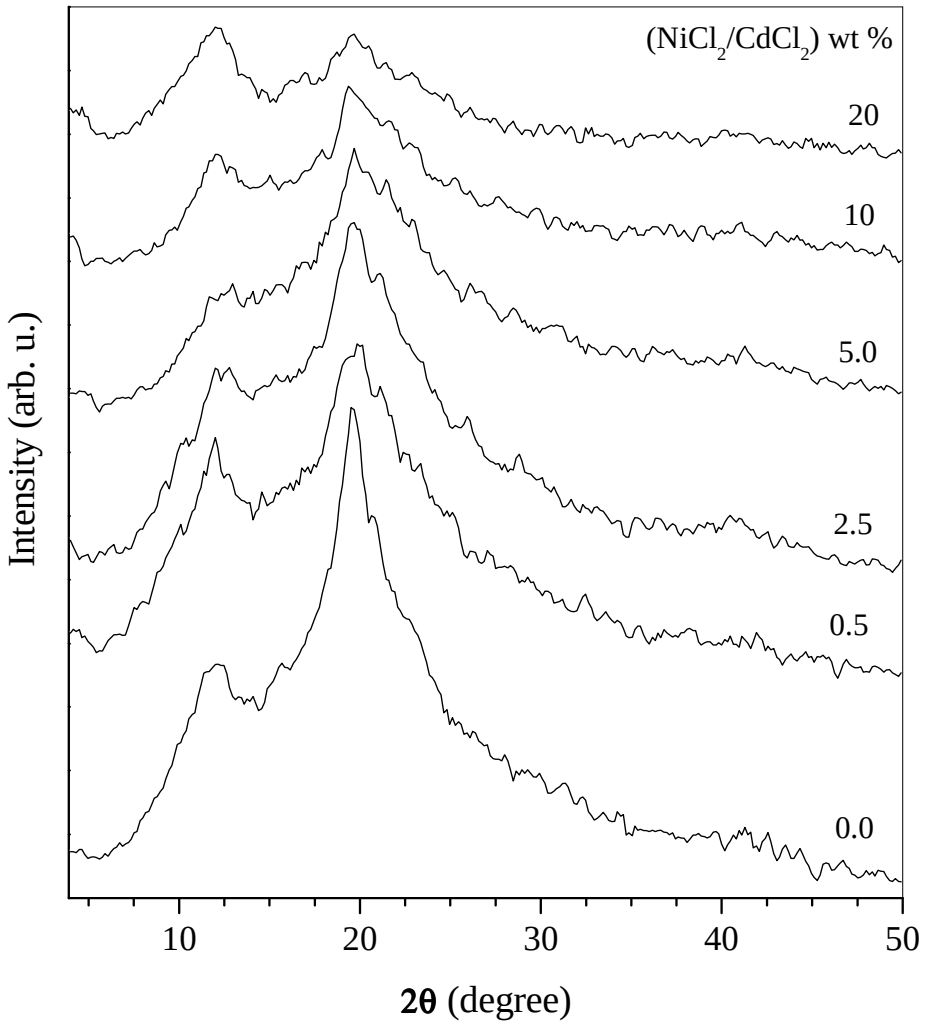

Fig. 1. X-ray diffraction of pure PVA/PVP (50/50) blend and the polymer blend filled with different concentrations of the mixed filler ($NiCl_2/CdCl_2$)

3.2 Fourier Transform Infrared Analysis

To confirm the complexation of pure blend and the blend filled with $NiCl_2/CdCl_2$, FT-IR spectroscopy has been used due to its ability to detect the intermolecular interaction between the polymer blend and its interaction with the mixed filler.

FT-IR absorption spectra of the present system recorded at room temperature in the range of 4000-400 cm^{-1} are shown in Fig. 2. The spectra exhibited characteristic bands of stretching and bending vibrations of OH, C–H, CH_2, C=O and C=C groups. These characteristic bands in the present spectra are assigned and listed in Table 1.

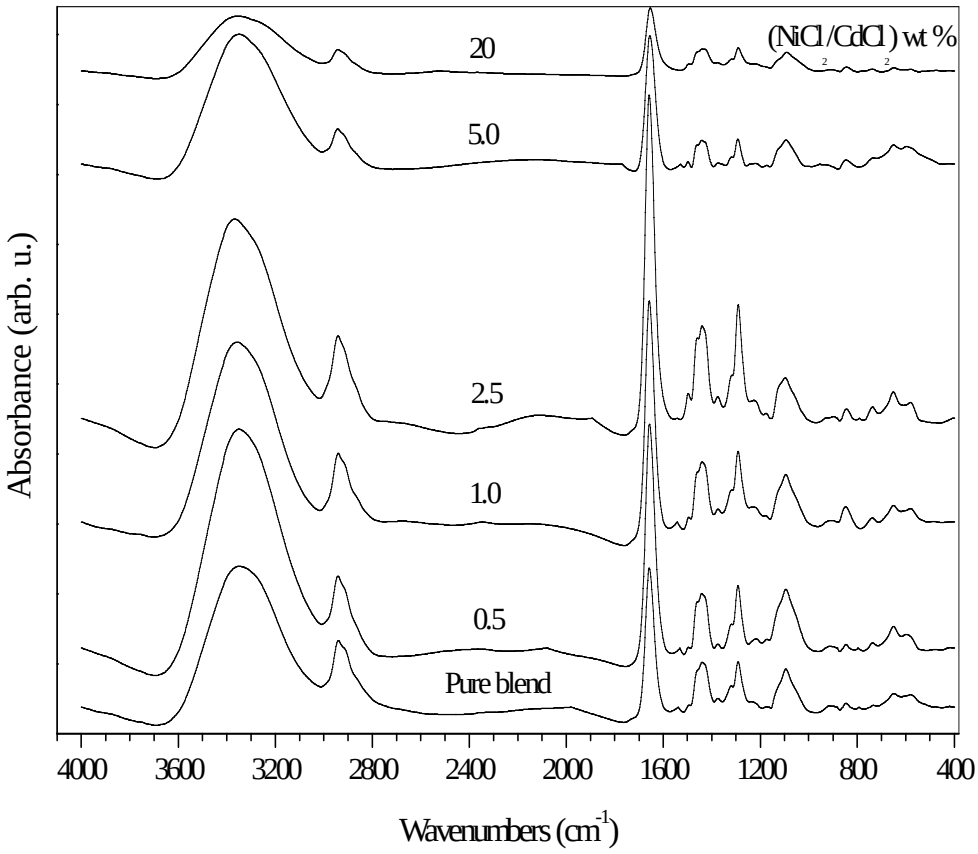

Fig. 2. FT-IR absorption spectra of the present system recorded at room temperature in the range 4000-400 cm^{-1}

From the spectra, the observed absorption band at about 3349 cm^{-1} is assigned to the stretching vibration of hydroxyl groups (OH) stemmed from the presence of PVA. This band became broader after adding the mixed filler as shown in this figure, where this is due to hydrogen bonds formation and due to the presence of Cl^- ions. This gives a clear indication about the specific interaction in the polymer matrices.

Another strong band observed at about 2940 cm^{-1} indicates an asymmetric stretching mode of CH_2 group [11]. The vibrational band at about 1657 cm^{-1} is assigned to C=O stretching which confirms the intermolecular interactions between the hydroxyl groups of PVA and carbonyl groups of PVP in the prepared films. It is remarkable that the present double bonds segments are considered as suitable sites for polarons and/or bipolarons [12]. Also, appearing of C=O stretching is due to the semicrystalline nature of the blend, which confirm

results of X-ray diffraction analysis. The two observed peaks at about 1374 cm^{-1} and 1439 cm^{-1} are assigned to CH_2 bending and scissoring vibrations, respectively. Because the vibration of the later, most influenced upon the coordination interaction between the carbonyl groups and ions was occurs [13].

Table 1. Assignment of the characteristic bands in the present spectra

Vibrational frequency (cm^{-1})	Band assignment
3349	OH stretching
2940	CH_2 asymmetric stretching
1657	C=O stretching
1539	C=N (pyridine ring)
1439	CH_2 scissoring
1374	CH_2 bending
1291	C–H wagging and/or C–N stretching
1224	C–C stretching and/or CH_2 deformation
1094	C–O stretching
913	out-of-plane rings C–H bending
845	C–H rocking
733	CH_2 rocking
579	C–Cl stretching

The vibrational sharp peak observed at about 1291 cm^{-1} may be attributed to C–N stretching of PVP [14], while the other weak band at about 845 cm^{-1} may be assigned to C–H rocking of PVA [15]. It is observed that intensities of the previous ed peaks increased for the concentrations ≤ 2.5 wt % and started to decrease for that > 2.5 wt % of the mixed filler content.

The observed small shifts in positions of some bands in the present spectra indicate the chemical interactions and complexation between $NiCl_2$/$CdCl_2$ and the polymer blend matrices [16].

3.3 UV-visible Analysis

UV-visible spectroscopy is useful as an analytical technique for two reasons. First, it can be used to identify some functional groups in molecules and secondly, it can be used for assaying (i.e. determining the content and strength of a substance).

UV-visible spectra in the wavelength range of 200-600 nm of the present samples recorded at room temperature are shown in Fig. (3). The spectra exhibit a weak band centered at about 208 nm, which can be assigned to $n \rightarrow \pi^*$ transition. During such transition in a molecule, electrons are promoted from the highest occupied molecular orbital (HOMO) to the lowest unoccupied molecular orbital (LUMO).

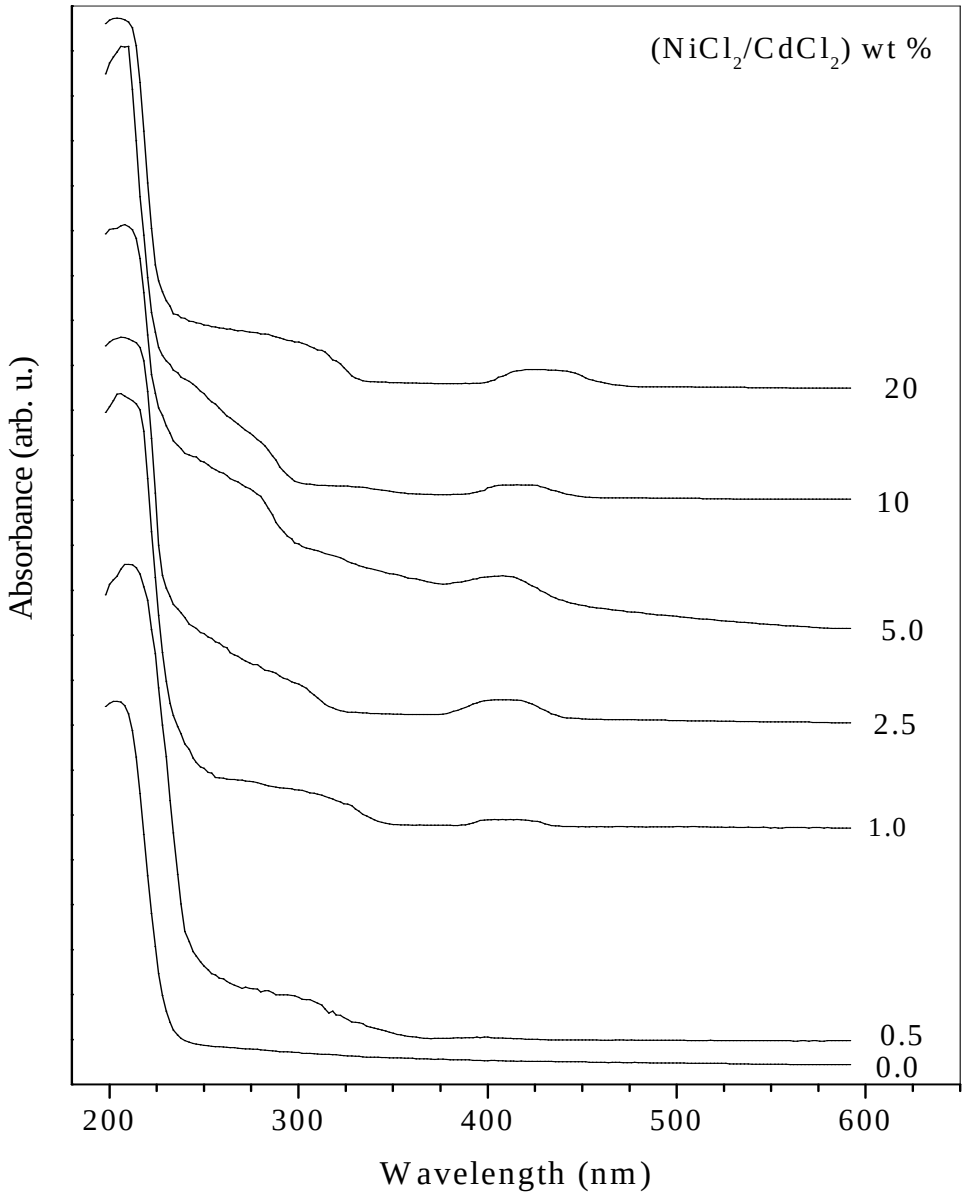

Fig. 3. UV-visible spectra in the wavelength range of 200-600 nm of the prepared samples recorded at room temperature

The presence of main absorption edge at about 218 nm is due to the semicrystalline nature of the samples. This absorption edge has small shift toward longer wavelengths with increasing the fillers content, indicating the complexation between all used components. This also may be attributed to change in crystallinity due to adding the mixed filler [17], which confirms XRD and FT-IR results.

The observed absorption shoulder centered at about 270 nm may be attributed to $\pi \rightarrow \pi^*$ which comes from unsaturated bonds, mainly; carbonyl groups (C=O and/or C=C) [6], which is responsible for electrical conduction in the samples. Another band observed at about 410 nm can be assigned to Ni-ions, where its intensity increased with increasing the mixed filler content. The appearance of this band confirms the occurrence of complexation between the fillers and blend. With increasing the mixed filler content, it is observed that this band is shifted toward higher wavelengths at about 430 nm.

The study of optical absorption gives information about the band structure of organic compound. Semiconductors are generally classified into two types: *a)* direct band gap and *b)* indirect band gap. In direct band gap, the top of the valence band and the bottom of the conduction band both lie at the same zero crystal momentum (wave vector). If the bottom of the conduction band does not correspond to zero crystal momentum, then it is called indirect band gap [2]. In indirect band gap, transition from valence to conduction band should always be associated with a phonon of the right magnitude of crystal momentum [18]. Davis and Shalliday [19] reported that near the fundamental band edge, both direct and indirect transitions occur and can be observed by plotting $(\alpha h\upsilon)^2$ and $(\alpha h\upsilon)^{1/2}$, respectively, as a function of energy ($h\upsilon$) (where h is Planck's constant). The analysis of Thutpalli and Tomlin [20] is based on the following relations:

$$(n\alpha h\upsilon)^2 = C_1(h\upsilon - E_{gd}) \quad (1)$$

$$(n\alpha h\upsilon)^{\frac{1}{2}} = C_2(h\upsilon - E_{gi}) \quad (2)$$

where, $h\upsilon$ is the photon energy, E_{gd} , the direct band gap, E_{gi} , the indirect band gap, n, integer, C_1 , C_2 , constants and α is the absorption coefficient. The absorption coefficient (α) can be determined as a function of frequency using the formula [21]:

$$\alpha(\upsilon) = 2.303 \times \frac{A}{d} \quad (3)$$

where, A is the absorbance and d is the path length of the quartz cuvette. The experimental data have been fitted with theoretical equations (1) and (2). As expected, the best fit is obtained for equation (2). This behaviour indicated that the transitions are indirect allowed transitions. So, we plot $(\alpha h\upsilon)^{1/2}$ versus photon energy ($h\upsilon$) in order to determine the optical band gap energies (E_g) by drawing the extrapolation of the straight portion of the curve to the $h\upsilon$-axis, i.e., at $\alpha = 0$. The optical band gap energy obtained in the present work is given in Table (2). From this table, values of E_g of the filled blend have been decreased, indicating that there are charge transfers complexes arose in the polymer blend (host lattice) by small amounts of Ni/Cd ions [22].

All curves are characterized by the presence of an exponentially decay tail at low energy. The tail of the absorption edge is exponential indicating the presence of localized states in the energy band gap, also indicating the presence of amorphous regions which correlated to the previous measurements. The origin of this band tailing is still a matter of conjecture but according to Dow and Redfield [23], it arises from the random fluctuations of the internal fields associated with structural disorder.

3.4 Differential Scanning Calorimetry

In order to get information about temperatures of the different phase transitions, DSC measurements have been carried out on the prepared samples. DSC also is one of the most convenient methods to determine miscibility and thermal properties of polymer blend [2].

The DSC thermograms obtained for pure and filled blend with different concentrations of the mixed filler are shown in Fig. 4. All samples were heated from ambient temperature to 450ºC at a heating rate of 10ºC/min under argon atmosphere. From this figure, the observed thermal transitions can be assigned as follows: The exothermic peak (T_w) at about 48ºC for all samples could be due to a small amount of moisture present in them unless it is carefully vacuum dried.

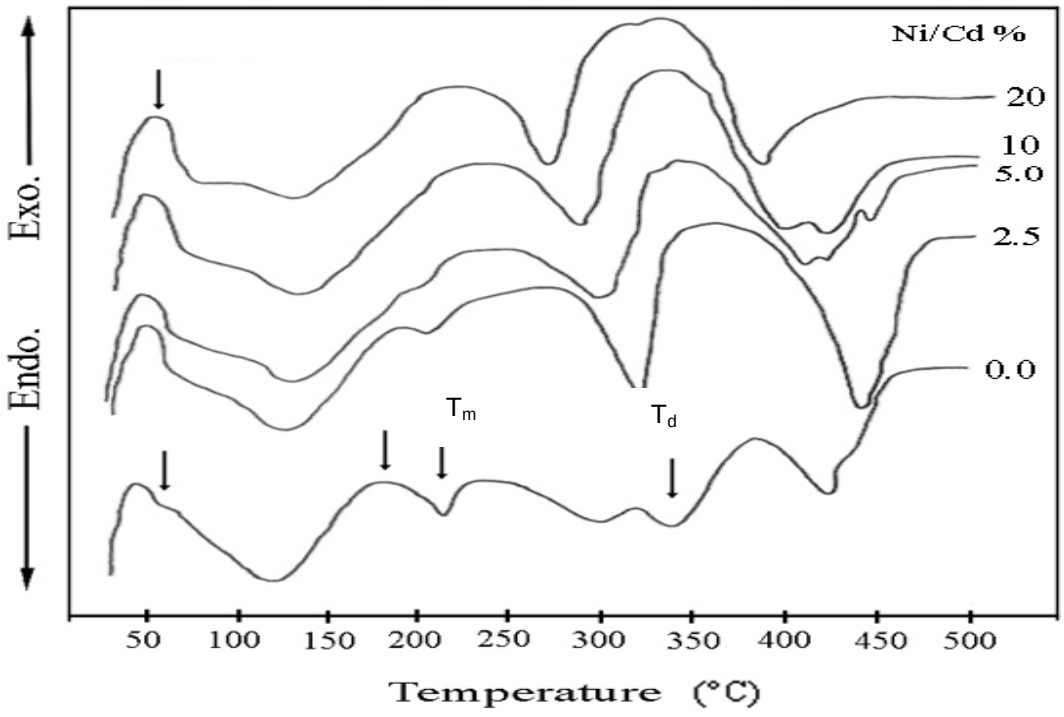

Fig. 4. DSC thermograms obtained for pure and filled blend with different concentrations of the mixed filler

The glass transition temperature (T_g) of pure PVA is about 53.3ºC and 170ºC for pure PVP [24,25]. Pure PVA/PVP blend curve shows a small single transition at about 64ºC attributed to T_g relaxation process resulting from micro-Brownian motion of the main chain backbone [6,25]. In general, DSC curve of a miscible polymer blend system shows a single T_g or melting peak, because the component polymer molecules would interact with each other [26]. This interaction would affect the crystallization and glass transition temperature of the blend. The presence of this single T_g indicates miscibility of the blend. This miscibility should be promoted by hydrogen bonding formation between hydroxyl groups of PVA and carbonyl groups of PVP.

The broad exothermic peak centered at about 175ºC was attributed to α-relaxation associated with the crystalline regions [27]. The position of α-relaxation temperature (T_α) was slightly shifted toward higher temperatures and its intensity decreased with increasing the mixed filler content. The change in the position of T_α might mainly have been due to the effect of filling on the orientation of crystals, crystallinity and micro-structure of the samples [28]. It is observed that it was disappeared at W ≥ 10 wt % and this may be due to its weakness and/or increasing the amorphous regions in the samples.

The endothermic peak observed at about 212ºC is assigned to melting temperature (T_m) and that at about 335ºC is assigned to decomposition temperature (T_d). The endothermic peak at about 420ºC may be assigned to second decomposition temperature (T_{d2}). It is clear that, the melting temperature decreased with the increase of $NiCl_2$/$CdCl_2$ content. This decrease of T_m (from 212ºC to 197ºC) suggests a large influence of the intercalation treatment of the polymer blend matrices.

The influence of filling on the enthalpy of fusion (H_f) of the present system was observed as shown in Table (2), where its values decreased with increasing concentrations of the mixed filler. This behaviour may be due to high viscosity of the prepared samples which makes crystallization more difficult. The tendency of an apparently disproportional decrease in H_f with increasing the fillers content implies a rapid decrease in the degree of crystallinity of the polymer blend component due to filling with $NiCl_2$ and $CdCl_2$. The sensitivity of H_f and T_m of the prepared samples indicates the presence of interaction between the mixed filler and the blend matrices.

Table 2. E_g, T_w, glass transition (T_g), melting (T_m), decomposition (T_d) temperatures and the enthalpy of fusion (H_f)

W (wt %)	E_g (eV)	T_w (ºC)	T_g (ºC)	T_m (ºC)	T_d (ºC)	H_f (μV. s/mg)
0.0	5.4	48	64	212	335	23.04
2.5	5.2	51	65	201	315	21.54
5.0	5.1	49	65	197	295	7.39
10	4.98	50	67.5	–	282	7.97
20	4.75	52	68	–	268	3.12

The position of T_d shifts toward lower temperatures from 335ºC to 268ºC indicating the formation of an intermolecular interaction between the polymer blend and mixed filler. This confirms the results obtained by X-ray, FT-IR and SEM studies.

3.5 DC Conductivity Studies

Fig. (5) shows the variation of log (σ) as a function of inverse absolute temperature for various concentrations of the mixed filler in PVA/PVP blend. From this figure, it is observed that, as the temperature increases, values of conductivity are increased for all the prepared samples. The conductivity behaviour does not show any abrupt jump with temperature. This indicates amorphous structure of the prepared films [29], which is confirmed from XRD study.

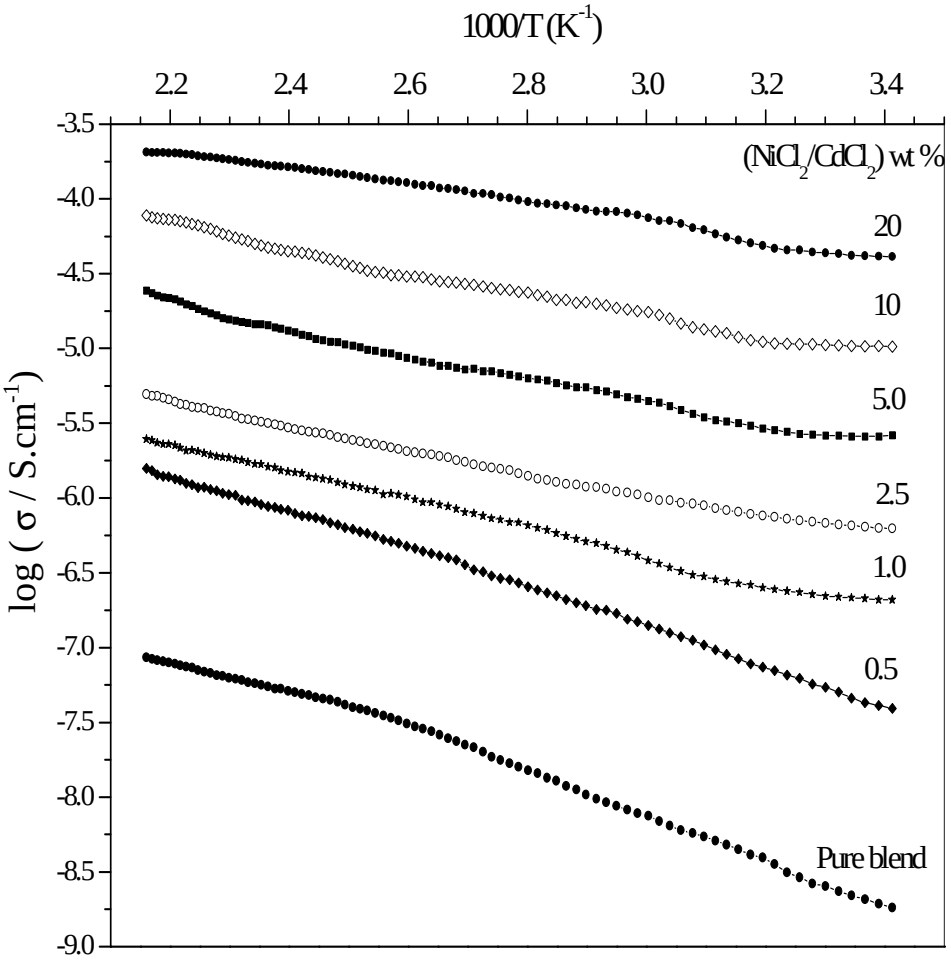

Fig. 5. The variation of log (σ) as a function of inverse absolute temperature for the present samples

This is in agreement with the free volume theory [30]. This theory is, at higher temperatures, thermal movement of polymer chain segments and the dissociation of fillers would be improved, which increased ionic conductivity for all complexes. As temperature increases, the amorphous polymer can expand easily, which results in an increase in the free volume of the system. Thus, the segmental motion either permits the ions to hop from one site to another or provides a pathway for ions to move. In other words, the segmental movement of the polymer facilitates the translational ionic motion.

Thus, ions, solvated molecules and/or polymer segments can move to the free volumes. So, according to this theory of polymers, when temperature is increased, the vibrational energy of a segment is sufficient to push against the hydrostatic pressure imposed by its neighboring atoms and create a small amount of space surrounding its own volume in which vibrational motion can occur [31]. An increase in temperature produces more free volumes,

which increases the mobility of ions and segments that will assist ion transport and practically compensate the retarding effect of the ion and hence conductivity [32]. It is clear that, no linear dependence obtained in the figure suggest that ion conduction follows Williams-Landel-Ferry (WLF) mechanism not Arrhenius [33]. Thus, the results may be effectively represented by the following equation [34]:

$$\sigma = AT^{\frac{-1}{2}} \exp\left(\frac{-E_a}{k(T-T_0)}\right) \quad (4)$$

where, E_a is related to the activation energy of ion transport associated with the configurationally entropy of the polymer chains, and its values are listed in Table (3). Thus, the non-linearity of the plots suggests that ionic transport in the samples is associated with the polymer segmental (i.e., polymer chain) motion.

Table 3. Values of activation energy of ion transport associated with the configurationally entropy of the polymer chains

W (wt %)	Activation energy (eV)
0.0	1.37
0.5	1.28
1.0	0.93
2.5	0.75
5.0	0.80
10	0.74
20	0.60

From Fig. (5), the conductivity was improved, where its values changed from (2.16 ± 1) × 10^{-8} S/cm of pure PVA/PVP blend to (1.1 ± 0.8) × 10^{-4}S/cm of the blend filled with 20 wt % of the mixed filler. These results suggest that this system can be used in some applications such as nickel/cadmium batteries.

3.5.1 Determination of the hopping distance (R_o)

It is well-known that, double-bond segments and structural defects (detected by FT-IR spectroscopy) are considered as suitable sites for the formation of polarons and/or bipolarons in the polymeric matrix. Therefore, the electrical conductivity can be expressed by [35]:

$$\sigma = \frac{Ae^2\gamma(T)^2}{kT}\frac{\zeta}{R_0^2}\frac{y_p y_{bp}}{(y_p + y_{bp})^2}\exp\left(\frac{-2BR_0}{\zeta}\right) \quad (5)$$

where, A= 0.45, B=1.39, y_p and y_{bp} are the concentration of polarons and bipolarons, respectively, R_o is the typical separation between impurities, $\zeta = (\zeta_{\parallel}\zeta_{\perp}^2)^{\frac{1}{3}}$ is the average decay length of a polaron and bipolaron wave function, $\zeta_{\parallel}$ and $\zeta_{\perp}$ are the decay lengths parallel and perpendicular to the polymer chain, respectively. Bredas et al. [36] reported that

the extension of defect should be the same for both polarons and bipolarons. The electronic transition rate between polaron and bipolaron states can be expressed as [35]:

$$\gamma(T) = 1.2 \times 10^{17} (T / 300K)^{n} \quad (6)$$

Where, n is a constant ≈ 11.

Using a computer-aided program, the order of magnitude of σ in the present system was adjusted with the impurity concentration, which actually was the fitting parameter. The parameters $\zeta_{\parallel}$ = 1.06 nm and $\zeta_{\perp}$ = 0.22 nm depend on the interchain resonance energy and the interchain distance. Taking $y_p = y_{bp}$ for simplicity, which is an acceptable approximation, using equations (5) and (6), we can obtain values of the hopping distance R_o.

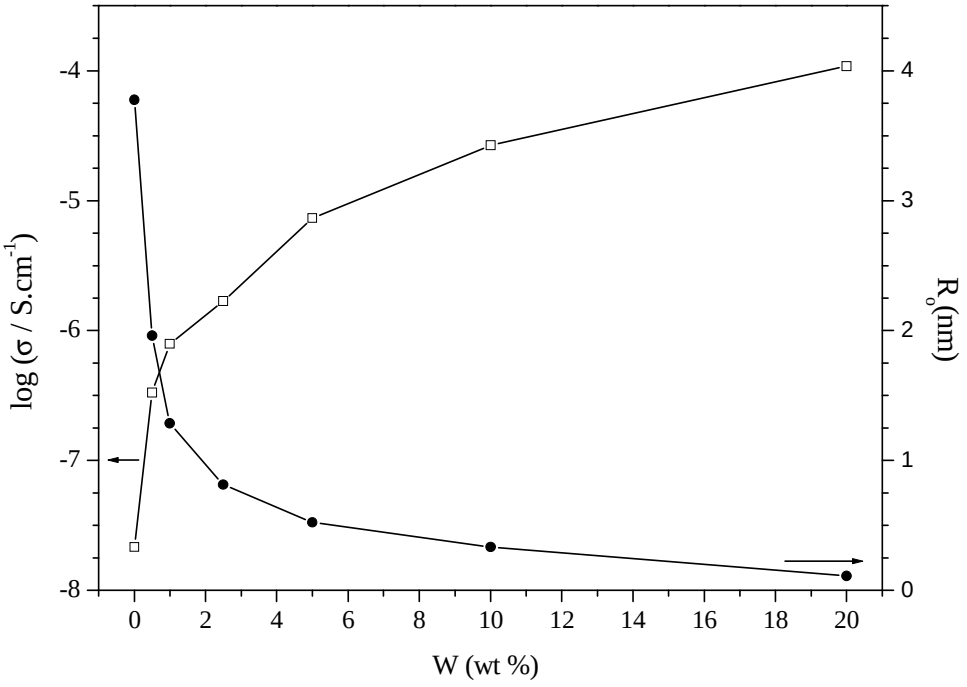

Fig. 6. The different concentrations of the mixed filler dependence on calculated R_o and log (σ) at constant temperature (T = 370 K)

It is remarkable that, the calculated values of R_o are in the range of 0.1-4.1 nm. Considering the monomer unit length to be ≈ 0.25 nm [37], it can be noticed that the hopping distance is of the 0.4-16.4 monomer unit lengths. This indicates that the present conduction mechanism is of an intrachain one-dimensional hopping type. Fig. 6 above shows the different concentrations of the mixed filler dependence on calculated R_o and log (σ) at constant temperature (T = 370 K). It is clear that R_o decreased while the conductivity was increased with increasing the concentration of the mixed filler, which suggest the choice of $NiCl_2/CdCl_2$ as mixed filler to improve the electrical conductivity of PVA/PVP blend.

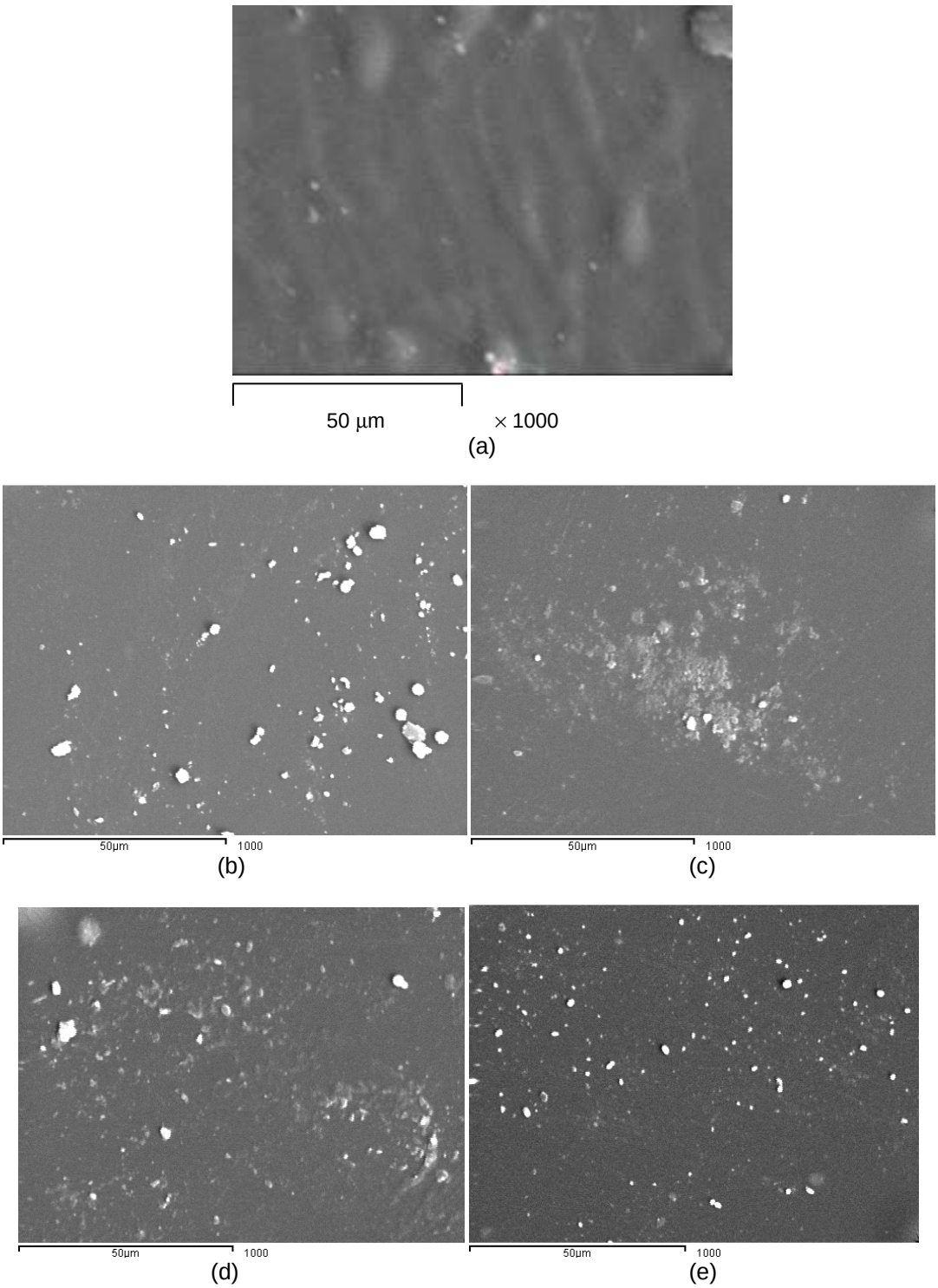

Fig. 7. SEM micrograph of the surface of: (*a*) pure blend, (b) 2.5, (c) 5, (d) 10 and (e) 20 % of the mixed filler at magnification 1000 times

3.6 Scanning Electron Microscopy

SEM is used to investigate fully the effect of the mixed filler content and the phase morphology of the films. Fig. 7 above shows the SEM micrograph of the surface of pure and filled polymer blend films at magnification 1000 times. The image of pure sample has a uniform surface morphology revealing a rather smooth surface.

For the filled samples, they have uniform surfaces, but there are semi-tori with different sizes in the range 1.39-4.17 μm. These semi-tori appeared as bright spots in all filled samples with different degree of roughness. The observed uniform distributed bright spots on the back-scattered images, as shown in the figure, seem to be agglomerates of the Ni/Cd particles, which increase with increasing the mixed filler content.

The degree of roughness of the surfaces increased with increasing $NiCl_2/CdCl_2$ contents. This indicates segregation of the mixed filler in the host matrix and this may be confirmed the interaction and complexation between the mixed filler and the polymer blend.

4. CONCLUSION

- PVA/PVP polymer blend pure and filled with different mass fractions of NiCl2/CdCl2 as mixed filler have been prepared by solution casting technique.
- XRD scans revealed increase in the amorphous regions inside the prepared samples with increasing Ni/Cd ions content. The complex formation in the polymer matrices has been elucidated in XRD, FT-IR and UV/visible studies.
- The relatively strong and weak bands appeared in FT-IR spectrum indicates the presence of stretching and bending vibrational modes of OH, C–H, CH2 and C=O groups.
- From UV-visible results, the main absorption edge at about 218 nm for all curves is attributed to the semicrystalline nature of the blend. Also, the decrease in values of the optical band gap of the filled blend indicates that there are charge transfers complexes arose in the polymer blend (host lattice) by small amounts of Ni/Cd ions.
- DSC study confirmed miscibility of the blend due to the presence of single glass transition temperature.
- The electrical conductivity was enhanced from 2.16 $\times$ 10-8 S/cm of pure polymer blend to 1.1 $\times$ 10-4 S/cm of the blend filled with 20 wt % of the mixed filler.
- Hence, PVA/PVP polymer blend filled with NiCl2/CdCl2 as mixed filler looks desirable and promising for fabrication of nickel/cadmium batteries.

COMPETING INTERESTS

Authors have declared that no competing interests exist.

REFERENCES

1. Utracki LA. Polymer Alloys and Blends-Thermodynamics and Rheology, New York: Oxford University Press; 1990.
2. Mohan VM, Raja V, Bhargav PB, Sharma AK Rao VVRN. Structural, electrical and optical properties of pure and $NaLaF_4$ doped PEO polymer electrolyte films.Journal of Polymer Research. 2007;14:283.

3. Makled MH, Sheha E, Shanap TS, El-Mansy MK. Electrical conduction and dielectric relaxation in p-type PVA/CuI polymer composite. Journal of Advanced Research. 2013;4:531.
4. Elashmawi IS, Abdelrazek EM, Hezma AH, Rajeh A. Modification and development of electrical and magnetic properties of PVA/PEO incorporated with $MnCl_2$. Physica B. 2014;4:57.
5. Shi Y, Xiong D. Microstructure and friction properties of PVA/PVP hydrogels for articular cartilage repair as function of polymerization degree and polymer concentration.Wear. 2013;305:280.
6. Eisa WH, Abdel-Moneam YK, Shabaka AA, Hosam AM. *In situ* approach induced growth of highly monodispersed Ag nanoparticles within free standing PVA/PVP films Spectrochemica Acta Part A: Mole. Biomol. Spect. 2012;95:341.
7. Abdelrazek EM, Elashmawi IS, El-Khodary A, Yassin A. Structural, optical, thermal and electrical studies on PVA/PVP blends filled with lithium bromide. Current Applied Physics. 2010;10:607.
8. Philips PJ. Electrical Properties of Solid Insulating Materials, ASTM Book Series of Engineering Dielectrics, ASTM. 1980;7.
9. Lee YM, Kim SH, Kim SJ.Preparation and characteristics of β-chitin and poly (vinyl alcohol) blend. Polymer. 1996;37:5897.
10. Hodge RM, Edward GH, Simon GP.Water absorption and states of water in semicrystalline poly (vinyl alcohol) films Polymer. 1996;37:1371.
11. Sweeting OJ. The science and technology of polymer films, New York. Interscience Publishers; 1968.
12. Tawansi A, El-Khodary A, Abdelnaby MM. A study of the physical properties of $FeCl_3$ filled PVACurrent Applied Physics. 2005;5:572.
13. Badr Y, Mahmoud MA. Manifestation of the silver nanoparticles incorporated into the poly vinyl alcohol matrices. Journal of Materials Science. 2006;41:3947.
14. Hao C, Zhao Y, Zhou Y, Zhou L, Xu Y, Wang D, Xu D. Interactions between metal chlorides and poly (vinyl pyrrolidone) in concentrated solutions and solid-state films.Journal of Polymer Science: Part B: Polymer Physics. 2007;45:1589.
15. Moharram MA, Khafagi MG. Application of FTIR spectroscopy for structural characterization of ternary poly(acrylic acid)–metal–poly(vinyl pyrrolidone) complexes. Journal of Applied Polymer Science. 2007;105:1888.
16. Bhargav PB, Mohan VM, Sharma AK, Rao VVRN. Investigations on electrical properties of (PVA:NaF) polymer electrolytes for electrochemical cell applications. Current of Applied Physics. 2009;9:165.
17. Abdelrazek EM, Elashmawi IS. Characterization and physical properties of $CoCl_2$ filled polyethyl-methacrylate films. Polymer Composites. 2008;29:1036.
18. Reddy CVS, Sharma AK, Rao VVRN.Electrical and optical properties of a polyblend electrolyte. Polymer. 2006;47:1318.
19. Davis DS, Shilliday TS. Some optical properties of cadmium telluride. Physical Review. 1960;118:1020.
20. Thutupalli GKM, Tomlin SG. The optical properties of thin films of cadmium and zinc selenides and tellurides. Journal of Physics D: Applied Physics. 1976;9:1639.
21. Kumar GNH, Rao JL, Gopal NO, Narasimhulu KV, Chakradhar RPS, Rajulu AV. Spectroscopic investigations of Mn^{2+} ions doped polyvinylalcohol films. Polymer. 2004;45:5407.
22. Abdelaziz M. Electron spin resonance and optical studies of poly(methylmethacrylate) doped with $CuCl_2$. Journal of Applied Polymer Science. 2008;108:1013.
23. Dow JD, Redfield D.Toward a Unified Theory of Urbach's Rule and Exponential Absorption Edges. Physical Review B. 1972;5:594.

24. Chrissafis K, Paraskevopoulos KM, Papageorgiou GZ, Bikiaris DN. Thermal and dynamic mechanical behavior of bionanocomposites: Fumed silica nanoparticles dispersed in poly(vinyl pyrrolidone), chitosan, and poly(vinyl alcohol). Journal of Applied Polymer Science. 2008;110:1739.
25. Seabra AB, Oliveira MG. Poly (vinyl alcohol) and poly (vinyl pyrrolidone) blended films for local nitric oxide release. Biomaterials. 2004;25:3773.
26. Ping ZH, Nguyen QT, Neel J. Investigations of poly (vinyl alcohol)/poly (N-vinyl-2-pyrrolidone) blends, 2. Influence of the molecular weights of the polymer components on crystallization. Makromolecules Chemei. 1990;191:185.
27. Zidan HM. Structural properties of CrF_3- and $MnCl_2$-filled poly(vinyl alcohol) films. Journal of Applied Polymer Science. 2003;88:1115.
28. Garrett PD, Grubb DT. Effect of drawing on the α relaxation of poly(vinyl alcohol). Journal Polymer Science Part B: Polymer Physics. 1988;26:2509.
29. Michael MS, Jacob MME, Prabaharan SRS, Radhakrishna S. Enhanced lithium ion transport in PEO-based solid polymer electrolytes employing a novel class of plasticizers. Solid State Ionics. 1997;98:167.
30. Linford RG. Electrochemical Science and Technology of Polymers, Elsevier Applied Science. London. 1987;3.
31. Armand MB, Chabagrs JM, Duclot MJ. In: Fast Ion Transport in Solids, Vasista P, Mundy JN, Shenoy G, (Eds.), North-Holland, Amsterdam. 1979;131.
32. Ramesh S, Ng KY. Characterization of polymer electrolytes based on high molecular weight PVC and Li_2SO_4. Current Applied Physics. 2009;9:329.
33. Williams ML, Landel RF, Ferry JD. The Temperature Dependence of Relaxation Mechanisms in Amorphous Polymers and Other Glass-forming Liquids. Journal of American ChemicalSociety. 1995;77:3701.
34. Plancha MJC, Rangeland CM, Sequeira CAC.ac conductivity of polymer complexes formed by poly (ethylene oxide) and nickel chloride. Solid State Ionics.1992;58:3.
35. Tawansi A, El-khodary A, Zidan HM, Badr SI. The effect of $MnCl_2$ filler on the optical window and the physical properties of PMMA films Polymer Testing. 2002;21:381.
36. Bredas JL, Chance RR, Silbey R. Physical Review B. Comparative theoretical study of the doping of conjugated polymers: Polarons in polyacetylene and polyparaphenylene. 1982;26:5843.
37. Wang YD, Cakmak M. Hierarchical structure gradients developed in injection-molded PVDF and PVDF–PMMA blends. I. Optical and thermal analysis Journal of Applied Polymer Science. 1998;68:909.

Peer-review history:
The peer review history for this paper can be accessed here:
http://www.sciencedomain.org/review-history.php?iid=630&id=5&aid=5774